A Fast Approach for Fusion of Hyperspectral Images through Redundancy Elimination

Ketan Kotwal* and Subhasis Chaudhuri
Electrical Engineering Department
Indian Institute of Technology Bombay
Mumbai, India
(ketan, sc)@ee.iitb.ac.in

ABSTRACT

The fusion of hyperspectral images is an important area in research and applications. Several fusion techniques have been developed in the literature for visualization of hyperspectral data. The amount of computation needed for such techniques is directly related to the volume of the data. Most of these techniques involve a significant amount of computation due to high volume of the data, making the fusion processes slow. We analyze the statistical characteristics of this data in order to develop a technique for faster fusion. The image bands in the hyperspectral data represent the response of the scene collected over contiguous narrow bands of wavelength. The adjacent bands being captured over neighboring wavelength bands, these images exhibit a very high degree of similarity. The fusion of these adjacent image bands, thus adds a very little amount of additional information. We exploit this redundancy in the data to provide a novel scheme for rapid visualization. We propose a scheme for the selection of a subset of images from a hyperspectral image cube that can produce fusion results with a very small amount of degradation in the quality compared to the quality of the result using the same technique of fusion applied over the entire data.

Keywords

Hyperspectral image fusion, image entropy, redundancy elimination

1. INTRODUCTION

The research in the area of hyperspectral image processing is of growing interest due to the distinct advantages offered by the hyperspectral images in terms of providing abundant information of the scene over a wide wavelength. The applications of hyperspectral image processing are being explored in various areas like, remote sensing, geological surveying, surveillance, and medical imaging [1, 2, 3]. Since the hyperspectral data contain around 200-250 images of the same scene acquired using narrowband sensors, visualization of these images is a difficult problem. Therefore, a computationally efficient technique of visualization of this rich source of information is one of the important steps in the processing of hyperspectral data for a quick overview and effective interpretation. However, due to a very large number of image bands, visualization of this data poses a challenging problem in image fusion in terms of computational costs and memory requirements.

Several image fusion techniques have been proposed in the literature for an efficient visualization of the hyperspectral data. The multi resolution analysis (MRA) based hyperspectral image fusion techniques have been analyzed for their performance in [4]. The principal component analysis (PCA) has been used as a classical tool for the dimensionality reduction. The hyperspectral fusion techniques based on the PCA are described in [5, 6]. However, due to a very high amount of computation, these techniques tend to be very slow in nature. Jacobson *et al.* [7] proposed a pixel based fusion technique by assigning fixed weights to each of the bands in the hyperspectral data, which are based on the certain optimization criterion for some of the commonly used color spaces. A bilateral filtering based technique for the visualization of hyperspectral data has been recently proposed [8], where a weight for each of the pixel in the data is uniquely defined to preserve the minor features during fusion. Some attempts for a quick visualization of the image contents in the form of an RGB image include the methods for selection of three image bands satisfying certain criteria [7, 9]. However, these approaches select only three bands for the display, and they do not involve any kind of image fusion. For the data level image fusion, available techniques evaluate the importance of a pixel within its spatial neighborhood, and then assign appropriate weights to the pixels while fusing them over various image bands. Since this step requires a significant amount of computation, usually on a per pixel basis, the time taken for the fusion is directly proportional to the number of image bands. Some of the pixel based techniques for the fusion of hyperspectral images are described in [4, 7, 8]. An observer has to wait until the completion of calculation of weights for the entire set of image bands, followed by the successive weighted addition to get the final result of fusion. Therefore, the fusion techniques tend to be slow due to the large number of image bands.

In this paper, we present a novel method for fast fusion of hyperspectral images. We provide an information theoretic

*Corresponding author

ICVGIP '10, December 12-15, 2010, Chennai, India

strategy for choosing specific image bands of the hyperspectral data cube. These selected bands can be fused using any existing and suitable pixel based fusion technique. Our contribution lies in providing a much faster scheme with a minimal degradation in the fusion quality.

2. PROPOSED APPROACH

In case of hyperspectral imaging sensors, these images are acquired over narrow but contiguous spectral bands typically about 10 nm, in the visible and infrared spectra. Therefore, the neighboring image bands in the hyperspectral data exhibit a very high degree of spectral correlation. Hence, when a fusion algorithm operates over two contiguous image bands, a very little additional information is contributed. Instead of processing the image bands in a sequential manner for the entire hyperspectral data set, a fewer number of image bands with higher amount of independent information can be fused to form a resultant image without much loss in the quality of the fused image. We propose a conditional entropy based approach for the selection of image bands which are mutually less correlated in order to facilitate a faster visualization. As the required quality of the fusion can be achieved using only a subset of image data, the proposed approach is essentially much faster and is memory efficient.

2.1 Redundancy Elimination

An image band to be fused with another should possess a significant amount of additional information for the fusion process to be efficient. We propose an algorithm to select the image bands based on conditional entropy. Initially the first band is selected for fusion, which acts as the reference. The conditional entropy of the successive image bands with respect to the reference band is then evaluated. The next band is selected when the corresponding conditional entropy exceeds a pre-determined threshold, i.e. when the additional information content in the given band is sufficiently high. The threshold is set to an appropriate fraction of the entropy of the band under consideration. The newly selected image band acts as the reference for the selection of the next image band to be fused. Thus, given a set of hyperspectral images $\{\mathbf{I}_j;\, j = 1, 2, \ldots, N\}$, and a reference image I_i, the k-th image band selected for fusion is given by,

$$k = \arg\inf_j \{H(I_j|I_i) \geq \theta\}, \quad j = i, i+1, i+2, \ldots \tag{1}$$

where $H(I_j|I_i)$ represents the entropy of the image I_j conditioned on the previously selected image I_i. The threshold θ is chosen as,

$$\theta = \alpha\, H(I_j), \quad 0 < \alpha < 1. \tag{2}$$

This procedure can be continued until the entire dataset is exhausted. Any pixel based fusion technique can then operate over this selected subset of the hyperspectral data to generate an appropriately fused image.

The proposed scheme exploits the statistical redundancy in the hyperspectral data. Therefore, although a fewer number of images are selected, most of the information content of the data is captured by the band selection process. The resultant fused image, thus, contains most of the features of the entire data. Further, since the method does not require all these bands to be read directly into the memory simultaneously, the method is also memory efficient.

2.2 Bounds on Computational Savings

In the proposed scheme, a band is selected if the entropy of the band conditioned on the reference band exceeds a threshold. Therefore, the number of bands being selected, and the corresponding average computational requirements in the proposed method depend on the distribution of the conditional information $H(I_j|I_i)$ of the image bands. Here we analyze savings in the computation on the basis of an appropriately chosen probability model. Since the term entropy involves an expectation operator, the corresponding quantity is a deterministic variable. We remove the expectation operator from H, and call it average information. For a given realization of the image, H may now be treated as a random variable.

Generally, the correlation between image bands decreases exponentially as the spectral distance between the corresponding bands increases, when we may use the following theorem to compute savings in the proposed technique.

THEOREM 1. *If the average conditional information $H(I_j|I_i)$ follows an exponential function with respect to the spectral distance with rate parameter λ, then the average saving in the computation is given by $S = \frac{\lambda}{\ln \frac{1}{1-\alpha}}$.*

PROOF. Let the conditional information be written as,

$$H(I_j|I_i) = H(I_j)\Big(1 - e^{-\lambda(j-i)}\Big), \quad j = i, i+1, i+2, \ldots \tag{3}$$

To obtain the computational savings, we use the expressions from Eq.(1)-(2) of the band selection process.

$$\begin{aligned} & H(I_j|I_i) = H(I_j)(1 - e^{-\lambda(j-i)}) \geq \alpha\, H(I_j), \\ \text{or,} \quad & 1 - e^{-\lambda(j-i)} \geq \alpha \\ \text{or,} \quad & j - i \geq \frac{1}{\lambda} \ln \frac{1}{1-\alpha} \end{aligned} \tag{4}$$

Thus, a band is selected if its spectral distance from the reference band exceeds the RHS of the Eq.(4). Therefore, the fractional savings (S) in computation is given by the inverse of above relation as,

$$S = \frac{1}{j-i} = \frac{\lambda}{\ln \frac{1}{1-\alpha}}. \tag{5}$$

□

The value of λ is dependent on the statistics of the hyperspectral data. A higher value of λ implies highly decreasing nature of the distribution of the conditional information. Thus, the computational saving is directly proportional to the rate parameter. Also, for very small values of α, there is practically no saving in computation, while higher values of α lead to very high values of the denominator in the expression, indicating a high amount of saving at the cost of selecting a very few image bands, thus sacrificing in the quality of the fusion results. The expression in Eq.(5) gives the theoretical upper bound on the computational savings. However, in practice, the computational savings are lesser due to the processing overhead of the calculation of the conditional information.

Now, we analyze the more interesting case of hyperspectral data by modeling the conditional information by an additional term that corresponds to the perturbation by an additive noise having a uniform distribution.

THEOREM 2. *If the average conditional information $H(I_j|I_i)$ as defined in Theorem 1 includes a perturbation by a white additive noise uniformly distributed in $[0,\ \beta]$, then the probability of band selection is given by* $\min\Big\{1 - \frac{H(I_j)}{\beta}(\alpha + e^{-\lambda(j-i)} - 1),\ 1\Big\}$.

PROOF. As defined, $H(I_j|I_i)$ is given by

$$H(I_j|I_i) = H(I_j)\big(1 - e^{-\lambda(j-i)}\big) + z \quad (6)$$
$$\text{where } z \sim U[0,\ \beta], \text{and typically } \beta \ll H(I_j).$$

Substituting the band selection criteria, we get

$$H(I_j)\big(1 - e^{-\lambda(j-i)}\big) + z \geq \alpha\, H(I_j)$$
$$\text{or,}\quad H(I_j)\big((1-\alpha) - e^{-\lambda(j-i)}\big) + z \geq 0$$
$$\text{or,}\quad z \geq H(I_j)\big(\alpha + e^{-\lambda(j-i)} - 1\big). \quad (7)$$

We denote $\upsilon = H(I_j)\big(\alpha + e^{-\lambda(j-i)} - 1\big)$. Then, the probability of band selection is given by,

Prob.(band j is selected, given i is the reference band)

$$= \frac{1}{\beta}\int_{\upsilon}^{\beta} dz = \min\big\{\frac{1}{\beta}(\beta - \upsilon), 1\big\}$$
$$= \min\Big\{1 - \frac{H(I_j)}{\beta}(\alpha + e^{-\lambda(j-i)} - 1),\ 1\Big\}. \quad (8)$$

□

The following corollaries may be deduced from Theorem 2.

COROLLARY 1. *In the limit $\beta \to 0$, Theorem 1 becomes a special case of Theorem 2.*

COROLLARY 2. *From Eq.(8), $\max(j-i) = \frac{1}{\lambda}\ln\frac{1}{1-\alpha}$, is same as that in Eq.(4). Hence, the maximum achievable savings factor in this case is also the same, i.e. $S_{max} = \frac{\lambda}{\ln\frac{1}{1-\alpha}}$. But Eq.(8) does not tell as how tight is the bound.*

COROLLARY 3. *If $H(I_j)$ is high, it can tolerate a proportionally larger perturbation β.*

3. EXPERIMENTAL RESULTS

To test the effectiveness of the proposed scheme, we have used two standard hyperspectral data sets provided by different sensors- the Hyperion and the AVIRIS. The data provided by the Hyperion consists of 242 image bands, while the AVIRIS sensor provides data in 224 bands. The preprocessing step removes bands having near-zero responses which is due to the molecular absorption of water and carbon dioxide [10]. After preprocessing, the number of useful bands reduces to nearly 200.

We have employed two different techniques of pixel based image fusion for the evaluation of the proposed scheme. We have tested the proposed scheme for a recent matte based fusion approach which uses a bilateral filter (BF fusion) [8]. Multiresolution based methods have always been preferred in the domain of image fusion [11]. An image fusion technique using discrete wavelet transform has also been used for the testing purposes (DWT fusion). In this technique, each of the constituent images is decomposed upto three hierarchical levels using the Haar wavelet. The low frequency components are averaged, while the high frequency components are fused using a weighted summation where the neighborhood energy acts as the weight. Our test results show that in both cases the fused images over the subsets of both of the test data, selected using the proposed conditional entropy based technique are comparable in quality to the resultant images generated over the fusion of entire dataset using the same algorithm.

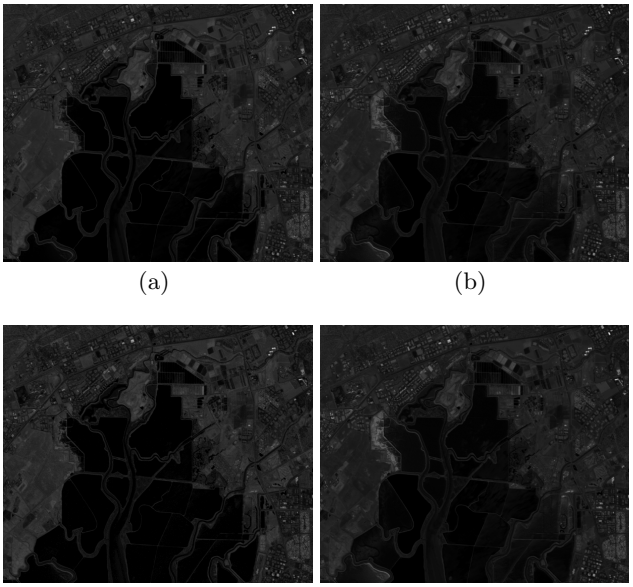

Figure 1: Results of fusion of the AVIRIS data applied over a subset of bands selected using the proposed approach. α was set to 0.50 and 29 bands were selected. (a),(c) show the results of BF fusion, and DWT fusion respectively, over selected bands. (b),(d) show the corresponding results of fusion of the entire data.

Fig.(1a) shows the result of fusion for the AVIRIS data using the Bilateral filtering based approach where only 29 selected image bands undergo the fusion. This figure may be compared to Fig.(1b) which represents the fusion of the entire hyperspectral data cube. It can be seen that Fig.(1a) retains most of the image features, and provides a visually comparable image quality. Similar results can be seen in Fig.(1c) which represents the fusion over a selected subset of 29 bands using the DWT-based technique. It may be compared to the corresponding Fig.(1d) where the entire dataset was used for fusion. These bands were selected using the proposed approach where the value of α was set to 0.50.

We also provide the performance evaluation of the proposed approach using some of the commonly used statistical parameters suggested in [12]. In Fig.(2), the entropy of the fused images as more and more bands are fused progressively, for various values of α can be seen, where the graph for $\alpha = 0$ corresponds to the fusion of entire data. For the fusion of selected 29 bands, corresponding to $\alpha = 0.50$, the entropy of the resultant fused image rises very rapidly, as compared to the fusion of entire dataset. Thus, using the proposed approach, it is possible to achieve fusion results in a very short time, with a little sacrifice in the image quality. Thus as α is increased there is more reduction in the computation. Thus Fig.(2) is also representative of the savings in

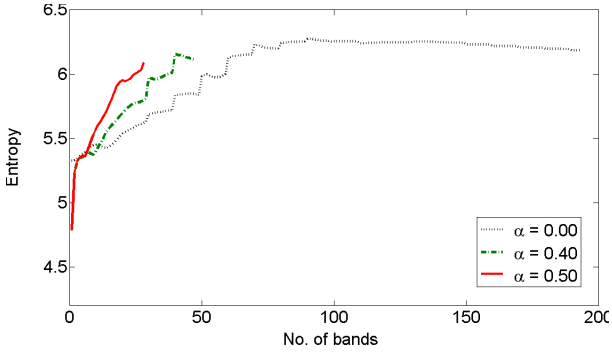

Figure 2: Performance evaluation of the proposed scheme for the number of bands required for effective fusion of Hyperion data for different values of α using BF fusion, and entropy as the criterion.

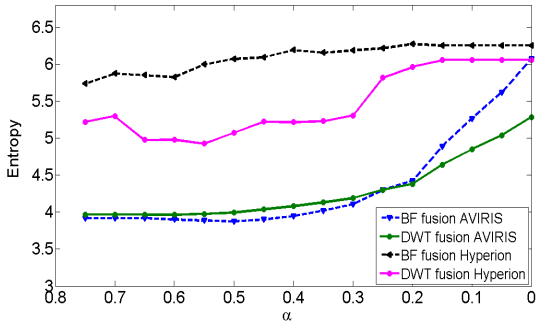

(a)

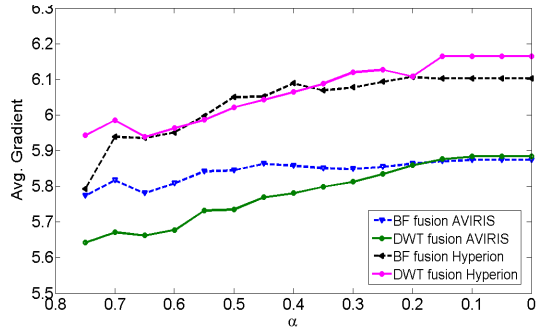

(b)

Figure 3: Performance evaluation of the proposed scheme using statistical parameters for various values of α. (a) and (b) show the variations in entropy and average gradient of the fused images for different values of α.

computation. It may be noted here that we assume the time to compute $H(I_j|I_i)$ is negligible compared to the fusion process, which is often true due to the common assumption of spatial memorylessness of individual bands while computing the entropy. Fig.(3a) shows the entropies of the fused images for different values of the threshold parameter α. It can be seen that for both the test data, the performance drops very slowly beyond a value of 0.30 for α signifying that an opportunity does exist to speed up the fusion process. An another performance measure based on the sharpness of the image of size (X, Y) can be defined as

$$\bar{g} = \frac{1}{XY} \sum_x \sum_y \sqrt{{I_x}^2 + {I_y}^2}. \quad (9)$$

This quantity $\bar{g}$, is called *Average gradient* which evaluates the quality of image by measuring its directional gradient in both the direction. We can make a similar observation from Fig.(3b) which shows the variation in the values of average gradient for various values of the threshold parameter.

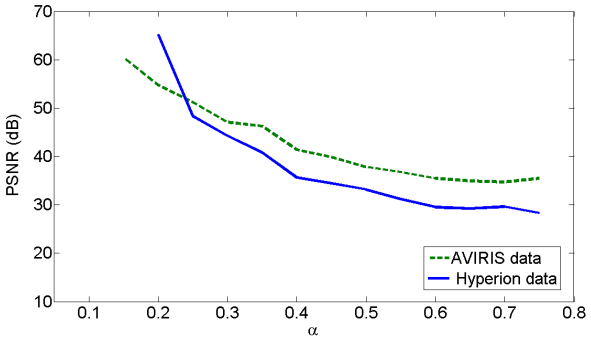

Figure 4: Plots of PSNR of the fused images for various values of α for the Hyperion and the AVIRIS data using the BF fusion technique. The resultant image from the fusion of the entire dataset used as a reference in each case.

In order to examine the quality of the fusion applied over a subset of images selected using the proposed scheme, we have analyzed the quality of the resultant fused images for various values of the threshold parameter α against the fused image resulting from fusion of the entire dataset using the same fusion method. This reference image is equivalent to the fusion of a subset selected with $\alpha = 0$. Fig.(4) provides the nature of the PSNR values of the resultant fused images using the Bilateral filtering based technique for various values of α where the fused image from the entire dataset using the same technique acts as a reference. For the values of α upto 0.15, all the image bands of the AVIRIS data were chosen for the fusion producing exactly the same result as the reference image, therefore the PSNR for these images does not exist. The PSNR values decrease as α increases indicating fewer bands are being selected. It can be seen that the resultant image with the fusion of 48 bands ($\alpha = 0.40$) gives visually almost similar results as the reference with PSNR more than 40 dB. Thus, a proposed technique can produce comparable results with only $^1/_4$-th of the dataset being selected for fusion purpose. A similar nature of PSNR plot can be observed for the Hyperion data in Fig.(4), where a bilateral filtering technique has been used for the fusion. A resultant image obtained from the fusion of a subset of 69 bands chosen by selecting α to be 0.45 was found to provide a PSNR of nearly 35 dB. The PSNR does not exist for the values of α less than 0.20, as the proposed scheme selects all the image bands in the hyperspectral dataset, and produces the same final result of fusion as the reference image. Similar plots were observed for other pixel based fusion techniques also. A visual comparison of the fusion results of the proposed approach can be carried out from Fig.(5) where the resultant images obtained from the fusion of selected subsets of the Hyperion data using BF fusion technique are shown. The images in Fig.(5a)–(5d) are obtained from the subsets

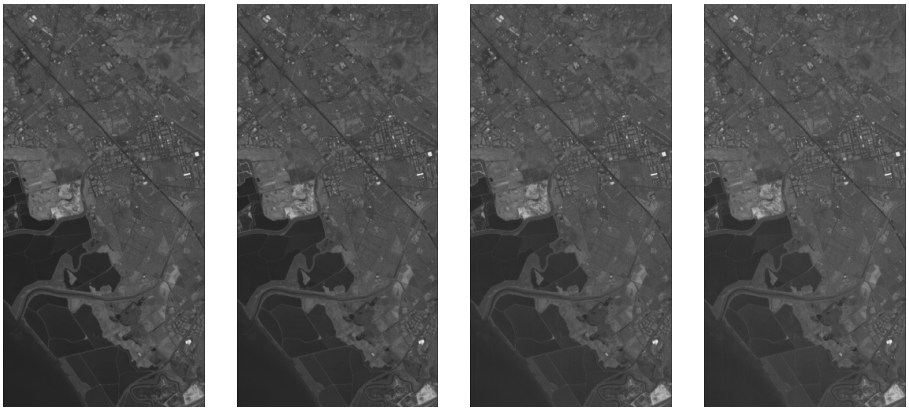

(a) (b) (c) (d)

Figure 5: Results of BF fusion of the Hyperion data applied over a subset of bands selected using the proposed approach. (a)-(d) show the results of fusion for α values 0.00, 0.35, 0.50 and 0.70, respectively.

of the Hyperion data of different cardinality by varying the threshold parameter. Fig.(5a) represents the fusion of the entire dataset, and thus it is considered as a reference for the evaluation purpose. Fig.(5b) is a result of the fusion of 108 selected bands of the data which reduces the computations nearly to the half of the original. Yet, the image does not produce any visible artifacts and gives a PSNR value of 41 dB when compared against the aforementioned reference. A result of the fusion of selected 55 bands was found to give 35 dB of PSNR [Fig.(5c)]. A set of 24 image bands was selected by choosing α to be 0.70. The resultant fused image is shown in Fig.(5d) which was found to give a PSNR of 30 dB for the fusion of approximately $^1/_{10}$-th of the data.

To quantify the closeness of fused images obtained over a subset to the resultant image from the fusion of entire dataset, we have also provided the analysis in terms of the Bhattacharyya distance. This distance metric measures the overlap between probability distributions of two images. As in the previous case, the resultant image from the fusion of entire dataset is considered as a reference. Fig.(6) provides the Bhattacharyya coefficient (BC) between the reference image and the resultant images obtained from the fusion of a subset of image bands for different values of α for the Hyperion as well as the AVIRIS data using BF fusion technique. In both the cases, the Bhattacharyya coefficient (BC) monotonically increases for increasing values of α which indicate reduction in the cardinality of the subset chosen for the fusion. The initial few values for BC are zero as the entire set of hyperspectral images was selected for the very small values of α.

The proposed scheme reduces a significant amount of computation and time, however it has an overhead of the calculation of the entropy of each image band. The proposed technique is beneficial only when the computation of actual fusion algorithm exceeds the computation of the entropy of each of the image band. However, except trivial and simple techniques like averaging, for most of the existing robust fusion techniques the time needed for band selection is much smaller than the time taken for the fusion of entire dataset. Therefore, the subset selection scheme proves to be highly effective for complex and computationally extensive techniques of fusion. The total computation W, taken for the pixel based fusion procedure as a function of threshold α, is

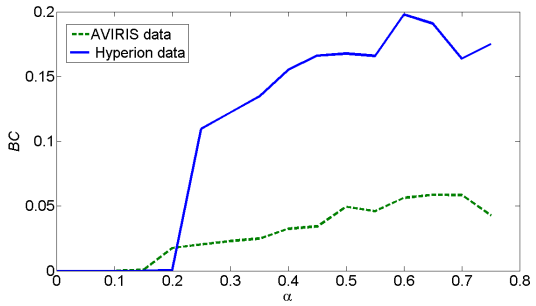

Figure 6: Plots of Bhattacharyya coefficient between the resultant image from the fusion of entire data and the resultant images from the fusion of subsets selected using the proposed approach for various values of α for the Hyperion and the AVIRIS data using the BF fusion technique.

of the form-

$$W(\alpha) = \gamma\, B(\alpha) + c_E$$

where $B(\alpha)$ represents the number of bands selected for a given threshold α, and c_E is the amount of computation for the evaluation of entropies of the image bands for the band selection procedure. This second term is a constant for a given dataset. The γ factor is a proportionality factor to account for a given fusion technique.

The amount of computation required for the fusion is linearly proportional to the number of images to be fused (i.e. $B(\alpha)$ here). Since the number of bands selected is inversely proportional to threshold, we may re-write the expression for computational time with an appropriately modified proportionality factor as-

$$W(\alpha) = \frac{\gamma'}{\alpha} + c_E. \tag{10}$$

For the quality based analysis of the proposed technique against the computational requirements, we have presented the plot of PSNR of fused images against the total time taken by varying threshold values. In Fig.(7) these plots for the Hyperion and the AVIRIS dataset are given for a BF fusion technique. A monotonically increasing nature of

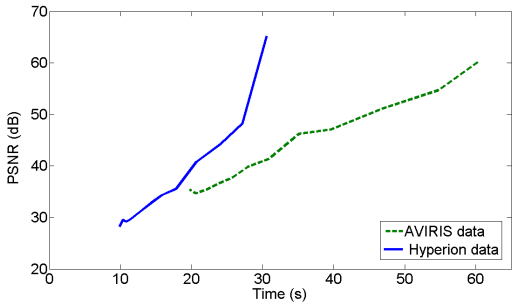

Figure 7: Plots of PSNR of the fused images against the timing requirements for the Hyperion and the AVIRIS data for the BF fusion technique. The resultant image from the fusion of the entire dataset used as a reference in each case for the evaluation of the PSNR.

these plots indicate the improvement in the quality of the fusion result at the expense of computational requirements.

4. CONCLUSIONS

We have proposed a novel information theoretic approach for the selection of specific image bands in the hyperspectral data. These selected bands are mutually less correlated, and thus they retain most of the information contents in the data. The fusion of this subset of hyperspectral data, therefore, is capable of representing most of the data features without any significant degradation in the quality. As only a fraction of the entire data is being fused, the proposed approach is computationally much faster. We have also provided a theoretical bound on how much computational savings can be achieved. An extensive performance evaluation of the proposed technique in terms of the quality of the subsequent fusion results, and computational time has also been presented.

5. ACKNOWLEDGMENTS

The funding supports from the Bharti Centre for Communication, and the J C Bose National Fellowship are gratefully acknowledged.

6. REFERENCES

[1] D. Landgrebe, "Hyperspectral image data analysis," *IEEE Signal Processing Magazine*, vol. 19, pp. 17–28, Jan 2002.

[2] H. Ren and C. Chang, "Automatic spectral target recognition in hyperspectral imagery," *IEEE Transactions on Aerospace and Electronic Systems*, vol. 39, pp. 1232–1249, Oct. 2003.

[3] T. Vo-Dinh, "A hyperspectral imaging system for in vivo optical diagnostics," *IEEE Engineering in Medicine and Biology Magazine*, vol. 23, pp. 40–49, Sep.-Oct. 2004.

[4] T. Wilson, S. Rogers, and M. Kabrisky, "Perceptual-based image fusion for hyperspectral data," *IEEE Transcations on Geoscience and Remote Sensing*, vol. 35, pp. 1007–1017, Jul. 1997.

[5] J. Tyo, A. Konsolakis, D. Diersen, and R. Olsen, "Principal-components-based display strategy for spectral imagery," *IEEE Transactions on Geoscience and Remote Sensing*, vol. 41, pp. 708–718, Mar. 2003.

[6] V. Tsagaris, V. Anastassopoulos, and G. Lampropoulos, "Fusion of hyperspectral data using segmented PCT for color representation and classification," *IEEE Transactions on Geoscience and Remote Sensing*, vol. 43, pp. 2365–2375, Oct. 2005.

[7] N. Jacobson, M. Gupta, and J. Cole, "Linear Fusion of Image Sets for Display," *IEEE Transcations on Geoscience and Remote Sensing*, vol. 45, pp. 3277–3288, Oct. 2007.

[8] K. Kotwal and S. Chaudhuri, "Visualization of Hyperspectral Images using Bilateral Filtering," *IEEE Transcations on Geoscience and Remote Sensing*, vol. 48, pp. 2308–2316, May 2010.

[9] B. Demir, A. Çelebi, and S. Ertürk, "A Low-Complexity Approach for the Color Display of Hyperspectral Remote-Sensing Images Using One-Bit-Transform-Based Band Selection," *IEEE Transcations on Geoscience and Remote Sensing*, vol. 47, pp. 97–105, Jan. 2009.

[10] R. A. Schowengerdt, *Remote Sensing - Models and Methods for Image Processing*. Academic Press, Inc., 3rd ed., 2007.

[11] J. J. Lewis, R. J. O'Callaghan, S. G. Nikolov, D. R. Bull, and N. Canagarajah, "Pixel- and region-based image fusion with complex wavelets," *Information Fusion*, vol. 8, no. 2, pp. 119 – 130, 2007.

[12] W. Cao, B. Li, and Y. Zhang, "A remote sensing image fusion method based on PCA transform and wavelet packet transform," in *Proceedings of International Conference on Neural Networks and Signal Processing*, vol. 2, pp. 976–981, Dec. 2003.